Chaotic dynamics in an Earth pointing, magnetically controlled spacecraft

Fabio Della Rossa and Fabio Dercole and Marco Lovera
Dipartimento di Elettronica, Informazione e Bioingegneria, Politecnico di Milano, Milan, Italy

Summary. The dynamics of a spacecraft equipped with magnetic actuators operating under a static attitude and rate feedback control law designed using averaging theory is considered and the asymptotic behavior of the closed-loop system is numerically analyzed, finding both the regions in which the control attains what desired and the regions in which it causes chaotic fluctuations of the spacecraft.

Introduction

Magnetic actuators have been studied extensively in recent years (see, *e.g.*, the survey [10]), as they represent a very attractive technology for attitude control (no moving parts, no propellant, high reliability). Unfortunately, the principle of operation of magnetic coils (control torques are generated by interacting with the magnetic field of the Earth) poses major challenges for control law design as it does not allow to provide three independent control torques at each time instant. In addition, these actuators are time-varying (almost-periodically forced), as the control mechanism hinges on the variations of the geomagnetic field along the spacecraft orbit. In spite of this, attitude stabilisation is possible as the system possesses average controllability properties for a wide range of orbit inclinations (see also [1]). Average controllability has allowed the derivation of almost global stability conditions for state feedback control laws achieving inertial pointing (see [7]) and Earth pointing (see [8]) for magnetically actuated spacecraft. Such results rely on averaging theory, *i.e.*, proceed by associating to the time-varying dynamics of the magnetically controlled spacecraft a time-averaged counterpart and showing that for sufficiently small values of a scaling parameter ε the trajectories of the former can be approximated by the ones of the latter. These results characterise the global properties of magnetic state feedback controllers, but leave open the problem of characterising the range of values of ε for which the results hold. In [3] (resp. [4]) local stability has been analyzed via bifurcation theory and a catalogue of other possible attractors for the range of practical interest of the parameter has been provided. This paper aims at investigating the dynamics of a magnetically actuated spacecraft under the state feedback control law of [7], for increasing values of ε, so as to characterize in a systematic way its chaotic behaviour and define the basins of attraction of the modes of operation of the feedback system.

Spacecraft model and control law

Only the case of a spacecraft in circular orbit with angular rate ω_0 is considered. Two reference systems are adopted: the orbital axes originate in the satellite centre of mass, the X-axis points to the Earth's centre, the Y-axis points along the orbital velocity vector and the Z-axis is normal to the satellite orbit plane; the satellite body axes originate in the satellite centre of mass and their axes are assumed to coincide with the body's principal inertia axes. Finally, in the following the unit vectors corresponding to the orbital axes will be denoted with e_x, e_y and e_z respectively, with the superscript ^{o} (^{b}) when considering the components of the unit vectors along the orbital (body) axes. The attitude dynamics of a spacecraft subject to gravity gradient can be expressed (in the body frame) as [11]

$$I\dot{\omega} = S(\omega)I\omega + 3\omega_0^2 S(Ie_x^b)e_x^b + T_{coils} \tag{1}$$

where $\omega \in \mathbb{R}^3$ is the vector of spacecraft angular rates, $I = \text{diag}[I_x, I_y, I_z] \in \mathbb{R}^{3\times 3}$ is the inertia matrix, $S(\cdot)$ is the skew-symmetric matrix operator associated with vector cross product ($a \times b = S(b)a$) and $T_{coils} \in \mathbb{R}^3$ is the vector of external torques induced by the magnetic coils. The relative attitude kinematics is given by

$$\dot{q} = \tilde{W}(q)\omega_r = \frac{1}{2}\begin{bmatrix} q_4 & -q_3 & q_2 \\ q_3 & q_4 & -q_1 \\ -q_2 & q_1 & q_4 \\ -q_1 & -q_2 & -q_3 \end{bmatrix}\omega_r \tag{2}$$

where $q = [q_1 \quad q_2 \quad q_3 \quad q_4]^T = [q_r^T \quad q_4]^T$ is the vector of unit norm Euler parameters (or quaternions, see, *e.g.*, [11]) and $\omega_r = \omega - \omega_t = \omega + \omega_0 e_z^b$ is the satellite angular rate relative to the orbital axes, in body frame. Letting $A(q)$ the attitude matrix relating the orbital and the body frames, one has that $e_x^b = A(q)e_x^o = A(q)[1 \quad 0 \quad 0]^T$, and similarly for e_y^b,e_z^b. The magnetic control torques are generated according to the law $T_{coils} = S(\tilde{b}^b(t))m_{coils}$, where $m_{coils} \in \mathbb{R}^3$ is the vector of magnetic dipoles for the three coils and $\tilde{b}^b(t) \in \mathbb{R}^3$ is the vector formed with the body components of the Earth's magnetic field. Note that $\tilde{b}^b(t)$ can be expressed in terms of $A(\boldsymbol{q})$ (see [11] for details) and of the magnetic field vector in the orbital frame, namely $\tilde{b}^o(t)$, as $\tilde{b}^b(t) = A(\boldsymbol{q})\tilde{b}^o(t)$. Since $\text{rank}\left(S(\tilde{b}^b(t))\right) = 2$, as mentioned in the Introduction magnetic actuators do not provide full controllability of the system at each time instant. Letting $\bar{q} = [0 \quad 0 \quad 0 \quad 1]^T$ (note that $A(\pm\bar{q}) = I$), the control problem consists in making the equilibrium $(q, \omega_r) = (\bar{q}, 0)$ of the closed-loop system locally exponentially stable and ensuring that almost all trajectories of the closed-loop system converge to the points $(q, \omega_r) = (\pm\bar{q}, 0)$. To this purpose the feedback control law $m_{coils} = \frac{1}{\|\tilde{b}^o(t)\|^2} S^T(\tilde{b}^b(t))\hat{\Gamma}_{av}^{-1}(\varepsilon^2 k_p q_r + \varepsilon k_v \omega_r)$ is applied, which leads to the closed-loop dynamics

$$\begin{aligned} \dot{q} &= \tilde{W}(q)\omega_r \\ I\dot{\omega} &= S(\omega)I\omega + 3\omega_0^2 S(Ie_x^b)e_x^b - \Gamma(t)\hat{\Gamma}_{av}^{-1}(\varepsilon^2 k_p q_r + \varepsilon k_v \omega_r), \end{aligned} \tag{3}$$

where $\Gamma(t) = S(b^b(t))S^T(b^b(t)) \geq 0$ and $b^b(t) = \frac{1}{\|\tilde{b}^b(t)\|}\tilde{b}^b(t)$. As for the geomagnetic field, a dipole approximation (see [9] for details) is considered.

Closed-loop system analysis

A preliminary analysis of the closed-loop system (3) was performed in [4], where the equilibrium $(\bar{q}, 0)$ was (numerically) shown to be asymptotically stable for increasing ε, though non-stationary attractors were detected even starting from initial

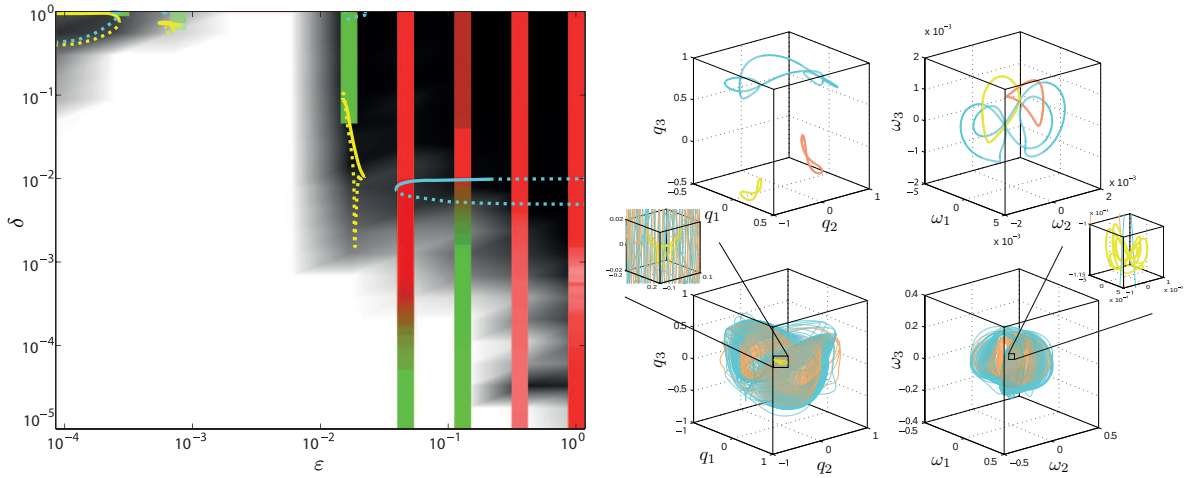

Figure 1: Numerical analysis of model (3), where the considered spacecraft has $I = \text{diag}[5, 60, 70]$ kg m^2, operates in a near polar (87^o inclination) orbit with an altitude of 450 km and a corresponding orbit period of about 5600 s. As for the control law, the scaling parameter ε varies, while $k_p = 500$ (A m^2), $k_v = 200$ A m^2/(rad/s).

conditions close to the equilibrium $(\bar{q}, 0)$. To estimate the basin of attraction of the equilibrium $(\bar{q}, 0)$, a two-parameter analysis w.r.t. the scaling parameter ε and the distance δ of the initial condition from the equilibrium was performed. As distance from an attitude q^1 to an attitude q^2, a measure of the angle (1 minus the cosine of half the angle) that rotates q^1 into q^2 by rotating around a suitable axis is considered (see, *e.g.*, [2] for a geometric interpretation of such a metric). Thus rotations of $\pm\pi$ give distance 1, though rotations of $\pm 2\pi$ give maximum distance 2. For each point of a grid over 10 values of ε (equally log-spaced in $[10^{-4}, 1]$) and 20 values of δ (equally log-spaced in $[10^{-5}, 1]$), we run 100 simulations of model (3) initialized with q at distance δ from $\bar{q}$ around a randomly selected axis and $\omega_r = 0$. For each simulation, we compute the associated Lyapunov exponents [5], thus adaptively eliminating the transient dynamics, and check whether if the equilibrium $(\bar{q}, 0)$ is reached. The white-to-black color code in Fig. 1 (left) indicates the fraction of the simulations reaching an alternative attractor. For each of those simulation, we plot a vertical bar covering the δ-values spanned by the reached attractor. The bar is green if the attractor is periodic (negative largest nontrivial LE), red if it is chaotic (positive largest LE), and is plotted with transparency, so the more are the simulations reaching the attractor, the more intense is the color. The white region at the bottom of Fig. 1 (left) confirms the local stability of the equilibrium $(\bar{q}, 0)$, though its basin of attraction vanishes for increasing ε. If the scaling parameter ε is too small, alternative periodic attractors can be reached, though large attitude perturbations from the equilibrium are required. Note that this not in contrast with Proposition 2 of [8], that ensures the almost global stability of the equilibrium $(\bar{q}, 0)$ for sufficiently small scaling ε and sufficiently large control gain k_p. Fig. 1 is in fact produced with a constant k_p (see caption), so that the control is too mild when ε is small. As expected, global stability is found for intermediate values of ε, whereas alternative periodic and chaotic attractors are present for larger ε. Note how the bars go close to $\delta = 0$ for increasing ε, that means that the fluctuating orbit in the attractor passes close to the equilibrium $(\bar{q}, 0)$. Thus, a stronger control destabilizes the closed-loop system, in the sense of reducing the basin of attraction of the desired equilibrium, and produces fluctuating attractors that are closer to it. Note, however, that the distance in state space from the equilibrium to the attractor is larger than what is shown in the figure, due to the velocity component ω_r, and in fact larger attitude perturbations at $\omega_r = 0$ are required to reach the attractor, as indicated by the white band at the bottom. Multiple attractors can be reached, as indicated by coexisting green and red bars and exemplified in the right part of the figure (multiple periodic attractors in the top panels, multiple periodic and chaotic attractors in the bottom panels). The solid (resp. dashed) lines indicate the min (yellow) and max (light blue) δ in stable (resp. unstable) periodic solutions, continued using orthogonal collocation techniques [6]. Note that multiple periodic solutions, as the yellow and orange ones in the top panels in Fig. 1 (right), are symmetric cycles at the same distance from the equilibrium $(\bar{q}, 0)$, so that they give the same continuation curve in Fig. 1 (left). Periodic solutions undergo several bifurcations, including fold, marking their appearance and disappearance, and period doubling and Neimark-Sacker, implying the loss of stability. Torus destruction is the observed cause for the appearance of chaotic attractors.

In conclusion, this analysis, to be possibly repeated for different values of the control gains, allows designers to tune the control law to guarantee the stability of the desired equilibrium and robustness to modeling and parametric inaccuracies.

References

[1] S.P. Bhat and A.S. Dham. Controllability of spacecraft attitude under magnetic actuation. In *IEEE Conference on Decision and Control*, 2003.

[2] N. A. Chaturvedi, A.K. Sanyal, and N.H. McClamroch. Rigid-body attitude control. *IEEE Control Systems*, pages 30–51, June 2011.

[3] F. Della Rossa, M. Bergamasco, and M. Lovera. Bifurcation analysis of the attitude dynamics for a magnetically controlled spacecraft. In *51st IEEE Conference on Decision and Control*, 2012.

[4] F. Della Rossa, F. Dercole, and M. Lovera. Attitude stability analysis for an Earth pointing, magnetically controlled spacecraft. In *Proceedings of the* 19^{th} *IFAC Symposium on Automatic Control in Aerospace*, pages 508–513, Würzburg, Germany, 2013.

[5] L. Dieci. Jacobian free computation of Lyapunov exponents. *Journal of Differential Equations*, 14(3):697-717, 2002.

[6] E. J. Doedel, A. R. Champneys, F. Dercole, T. F. Fairgrieve, Yu. A. Kuznetsov, B. Oldeman, R. C. Paffenroth, B. Sandstede, X. J. Wang, and C. H. Zhang. AUTO-07p: Continuation and bifurcation software for ordinary differential equations. Montreal, QC, 2007.

[7] M. Lovera and A. Astolfi. Spacecraft attitude control using magnetic actuators. *Automatica*, 40(8):1405–1414, 2004.

[8] M. Lovera and A. Astolfi. Global magnetic attitude control of spacecraft in the presence of gravity gradient. *IEEE Transactions on Aerospace and Electronic Systems*, 42(3):796–805, 2006.

[9] M. Psiaki. Magnetic torquer attitude control via asymptotic periodic linear quadratic regulation. In *AIAA Guidance, Navigation, and Control Conference*, 2000.

[10] E. Silani and M. Lovera. Magnetic spacecraft attitude control: A survey and some new results. *Control Engineering Practice*, 13(3):357–371, 2005.

[11] J. Wertz. *Spacecraft attitude determination and control*. D. Reidel Publishing Company, 1978.